Sphinx Journal of Pharmaceutical and Medical Sciences, Vol. 5, Issue 1, 2023, pp. 33-46.

SJPMS

Sphinx Journal of Pharmaceutical and Medical Sciences

e-mail: sjpms@sphinx.edu.eg

SPHINX UNIVERSITY

SILVER NANOPARTICLES WITH DIFFERENT COATING AGENTS: SYNTHESIS, CHARACTERIZATION AND LOADING WITH ROUSVASTATIN CALCIUM

Ahmed Sayed Ibrahim[1*], Ahmed El-Sayed Aboutaleb[2], Mahrous Osman Ahmad[2,3] and Jelan Abdel-Razik Abdel-Aleem[2]

[1]*Department of Pharmaceutics, Faculty of Pharmacy, Sphinx University, New Assiut 10, Assiut, Egypt*
[2]*Department of Industrial Pharmacy, Faculty of Pharmacy, Assiut University, Assiut 71526, Egypt*
[3]*Dean of Faculty of Pharmacy, Mirit University, New Sohag 82511, Egypt*

This work was conducted with the aim of formulating the antihyperlipidemic statin; rousvastatin calcium (RVC) using silver nanoparticles (AgNPs) as a carrier. The probability of the occurrence of interaction between RVC and the excipients used in synthesizing AgNPs was investigated using differential scanning calorimetry (DSC) and Fourier transfer infrared spectroscopy (FT-IR)). Silver nanoparticles (AgNPs) were synthesized using different capping agents; PEG 6000, sodium alginate, polyvinyl alcohol (PVA), β-cyclodextrin (β-CD), hydroxylpropyl-β-cyclodextrin (HPβ-CD) and Polyvinylpyrrolidone K90 (PVPK90). The silver nitrate was reduced using sodium borohydride. The formed AgNPs were then characterized by measuring their size and zeta potential and transmission electron microscopy (TEM). The results of DSC and Ft-IR revealed the absence of interaction between the used excipients and RVC. The loading capacity of AgNPs toward RVC was found to be dependent on the capping agent. The characterization of AgNPs by zeta analyzer shown the particle size diameter ranged from 184.7 to 812.1 nm depending on the capping agent. The values of zeta potential ranged from -32.8 to -10.5 Mv.

Keywords: Silver nanoparticles – rousvastatin calcium – drug-excipient compatibility – chemical synthesis of silver nanoparticles – nanoparticles characterization – encapsulating efficiency.

INTRODUCTION

Nanoparticle systems are widely investigated for their superior physical, chemical, and biological properties. A proper understanding of these systems is important for maximizing the benefits and potential of their applications. Silver nanoparticles (AgNPs) represent one of the most explored classes of nanomaterials particularly for new and improved antibacterial and antiinflammatory effects. This has find many applications in the pharmaceutical and cosmetic industry, anti-infective therapy and wound care, food and the textile industry[1-4]. Their extensive and versatile applicability relies on the genuine and easy-tunable properties of nanosilver; including remarkable physicochemical behavior, exceptional antimicrobial efficiency, anti-inflammatory action and antitumor activity[5&6].

AgNPs can be obtained by various top-down processes as evaporation-condensation processes of the bulk silver[7&8] and bottom-up processes as electrochemical interactions of

Received in 20/4/2023 & Accepted in 25/5/2023

*Corresponding author: Ahmed Sayed Ibrahim, E-mail: chessman6156@gmail.com

silver salts[9&10]. Their versatility and acceptable bio-functionality enabled the development and clinical implementation of several human-safe commercial products[11].

Despite many methods have been used in preparing AgNPs, the chemical reduction of silver nitrate has attracted much attention. Many studies reported the importance of surface coating on the bioavailability and toxicity of nanosilver. AgNPs modified with silicate and PVP neutral coatings induced less inflammatory effects and genotoxicity than negatively charged citrate and positively charged branched polyethylenimine (PEI) coatings[12]. In addition, Zelikin and coworkers[13] showed that 80 nm AgNPs coated with branched PEI were internalized and accumulated at a greater rate by epithelial cells, in comparison with nanoparticles coated with citrate, PEG, or PVP, causing significant mitochondria damage. In general, chemically synthesized spherical AgNPs showed stronger bactericidal effects than rod-shaped counterparts when used against both Gram-negative and Gram-positive pathogens. There is some evidence that the antibacterial activity of nanosilver is strongly related to their microstructure[14].

In addition to their intrinsic antibacterial activity, AgNPs proved noncable synergistic effects in the case of combined treatment with different natural or synthetic compounds. The treatment with PVA-capped nanosilver and hydrogen peroxide showed rapid and synergistic bactericidal effects against both Gram-negative and Gram-positive strains[15]. In comparison with conventional PVP-capped AgNPs, curcumin-capped nanosilver exert enhanced antibacterial activity. The presence of curcumin was thought to have superior penetrability of the bacterial cells and higher release of silver ions, resulting in ROS-mediated (reactive oxygen species) cytotoxicity[16]. Numerous examples from the literature demonstrate the effects of varying the shape, size, method of preparation, and excipients used in preparing AgNPs on their antibacterial and antiviral activity.

Tawfeek *et al.*[17] have concluded that functional coating of AgNPs with chitosan promoted their hepatic selectivity and biotolerability and considered these results as potential development of drug delivery systems for the treatment of liver diseases. A study on the retardation of bacterial biofilm formation by coating urinary catheters with AgNPs stabilized by coating with ethylcellulose (EC), polyvinylpyrrolidone (PVP) and polyethylene glycol (PEG) has been recently published[18]. The data obtained in this study provide evidence that AgNP-coated EC and PVP could be useful as potential antibacterial and antibiofilm catheter coating agents to prevent the development of urinary tract infections caused by E. coli. AgNPs which have been stabilized with either EC or Hydroxypropylmethyl cellulose (HPMC) showed a more pronounced antibacterial effect on Gram-negative bacterial species such as Pseudomonas aeruginosa, Salmonella typhimurium, and Serratia marcescens compared with the tested Gram-positive bacterial species[19].

The anti-inflammatory/antibacterial effects of statins like atorvastatin, simvastatin, fluvastatin, pitavastatin, lovastatin and pravastatin have been extensively reviewed[20&21]. However, few reports have dealt with the anti-inflammatory and antimicrobial activity of rousvastatin. The effects of RVC on carrageenan induced rat paw odema have been investigated[22]. It has been shown that oral administration of RVC apart from having lipid lowering activity, has got anti-inflammatory and antileukocyte accumulation activities inthe induced rat paw odema Albino rats models. Alagic-Dzambic *et al.*[23] investigated the activity of RVC against some bacterial/fungal spices. The authors concluded that the drug has *in-vitro* antimicrobial and antifungal effects.

In the present study AgNPs were prepared using different capping agents. The nanoparticles were characterized as per shape, size, and zeta potential. Furthermore, the different prepared AgNPs encapsulating efficiencies for RVC were determined.

EXPERIMENTAL

Materials

Polyethylene glycol 6000 (PEG6000), Polyvinyl alcohol (PVA), polyvinylpyrrolidone K90 (PVPK90), β-cyclodextrin (β-CD), hydroxylpropyl-β-cyclodextrin (HPβ-CD) were purchased from Aldrich Chem. Co. (USA), sodium borohydride ($NaBH_4$) was purchased

from SD Fine-Chemicals Limited (India). Silver nitrate ($AgNO_3$) was purchased from Alpha Chemicals (Cairo, Egypt), rousvastatin calcium (RVC) was purchased from Carbosynth Limited (UK).

Equipment

Electric balance, Sartorius TE214S, Germany-Differential scanning Calorimeter DSC-50, Shimadzu, Japan - Fourier transform Infrared (FT-IR) spectrophotometer, Nicolet 6700 FT-IR, Thermo Fisher, Madison, USA - Scanning electron microscope, SEM (JEOL TEM Model 100 CXII, Tokyo, Japan. UV-VIS double beam spectrophotometer, PerkinElmer, lambda25 UV–Vis Spectrophotometer - Nanotrac Wave II, Microtrac, USA - Zetasizer Nano ZS, Malvern Instruments, Worcestershire, UK.

Methods

Fourier Transform Infrared (FTIR) Spectroscopy

Samples (Approx. 3 mg) of the individual substances, as well as the physical mixtures (1:1 w/w) of RVC and the investigated excipients (β-cyclodextrin, Hyrroxypropylβ-cyclodextrin, sodium alginate, polyethylene glycol 6000, Polyviylpyrrolidone K90 and polyvinyl alcohol) prepared by mixing of the ingredients on a clean waxy paper for at least 4 minutes, then were remixed with potassium bromide. The mixture was compressed into discs in the IR compressor unit under vacuum. The discs scanned from 4000-400 cm^{-1} with an empty pellet holder as a reference.

Synthesis and coating of AgNPs

Synthesis and coating of AgNPs can be done in one step with some modifications of the previously reported methods[24]. Two ml of 1 mM silver nitrate solution was added to 48 ml of 1% w/v concentrations of each of the capping agents and stirred for 15 min under dark conditions since AgNPs are quite sensitive to duration and intensity of light exposure. Two mM of sodium borohydride was added drop-wise until the solution color turned yellow. Afterward, the solutions were centrifuged at 12,000 rpm for 15 min. Finally, the NPs were re-dispersed in deionized water and stored in the dark at 4°C.

Loading of silver nanoparticles with rousvastatin calcium

Coated AgNPs were mixed with 1 ml of 0.5mg/ml RVC solution prepared by dissolving the drug in minimum volume of methanol and dilution with double distilled water. Each mixture type was made as triplicates. All mixtures were shaken in a rotary shaker at 37±0.5°C for 24 hrs[25&26] and then incubated at 4°C in dark conditions.

The mixtures were centrifuged for 15 min at 12,000 rpm. After that, the supernatants were assayed using UV-VIS spectroscopy at λ_{max} of 242 nm to determine the amount of free RVC. Subsequently, the drug encapsulation efficiency % (EE) was calculated by subtracting the sum of the final drug concentration in the supernatant solution and the wash from the initial drug concentration in the initial solution as shown in Equation 1[26].

EE % = (Initial amount of RVC - Supernatant free RVC) / (Initial amount of RVC) x 100

Eq. 1

RESULTS AND DISCUSSION

Drug-excipients compatibility studies

DSC and FT-IR spectroscopy techniques were used to detect the possible interactions between RVC and the investigated excipients. The drug and the chosen excipients must be physically and chemically compatible. These techniques are frequently used to predict any possible interactions that would take place on situ or during the shelf life of the formulations.

In DSC, these incompatibilities could be detected by the appearance, shift, disappearance of the endothermic or exothermic peaks and/or variations in the corresponding relevant values of enthalpy in the thermograms of drug-excipient mixtures[27]. Differential scanning calorimetry determines the amount of heat absorbed or released by a substance when it is subjected to a constant temperature and for a given time resulting in an endothermic or exothermic process. First, it was necessary to study the behaviorof the API and each of the excipients individually.

The DSC-thermogram of RVC exhibits a short endothermic peak located at 143°C (Fig. 1B). The results revealed temperatures like

those reported in the literature9, preceded by an endothermic process at 72.25°C due to water loss.

The same applies to the early endotherm in HP-βCD. A weak endothermic peak is observed at 143°C due to the melting of RVC. The endothermic peak observed at 123°C for the mixture was weaker due to RVC melting in its physical mix with HP-βCD (Fig. 2). This shift in melting point and lesser ΔH me be attributed to the dilution effect of RVC by the cyclodextrin. The possibility of complex formation also exists.

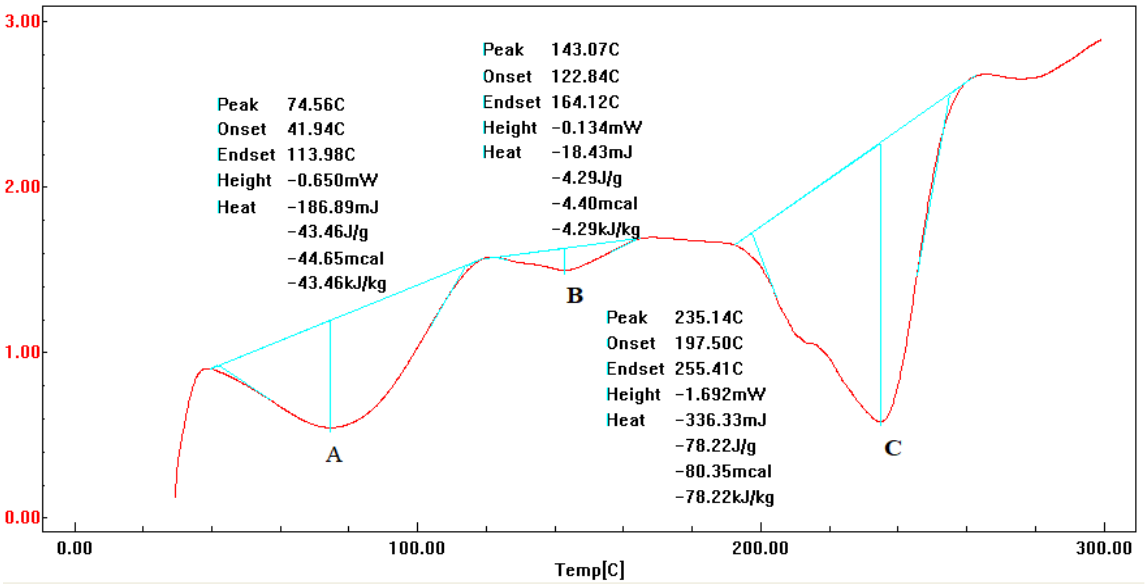

Fig. 1: Detailed DSC thermogram of rousvstatin calcium, A: water loss, B: Melting peak, C: Decomposition of RVC.

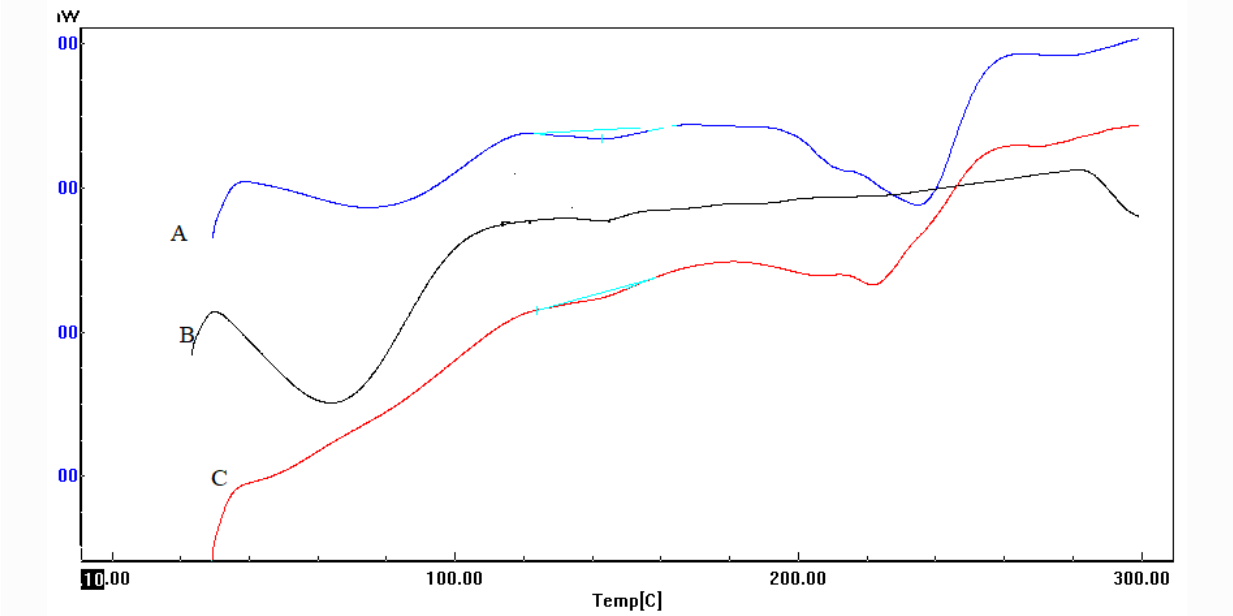

Fig. 2: DSC Thermograms of A: Rousvastatin calcium, B: HP-βCD and C: physical mix of A and B.

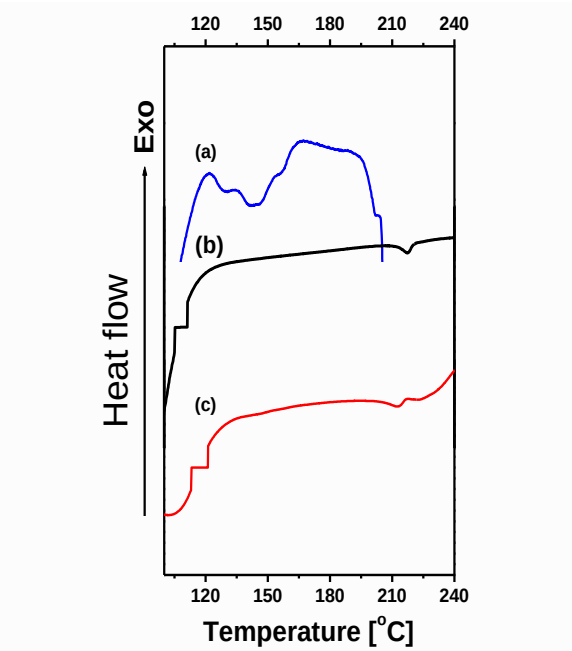

Fig. 3: DSC Thermograms of a: rousvastatin calcium, b: β-CD and c: physical mix of a and b.

In figure 3, the scale was changed with the curves drawn using the data of the Excel sheet provided by the DSC instrumentation in order to magnify any peak due to RVC in the mixture with β-CD. The absence of the drug peak strongly suggests formation of complex.

The FT-IR spectrum of RVC powder is shown in figure 4. The results reveal identical spectra for the tested powder and the reference[28]. Where, characteristics peaks of 2968.55 cm^{-1} for N-H stretching and C=O stretching of acid at 1732.13 cm^{-1}.

The other principle peaks are at 1548.13 cm^{-1} for C=C stretching, 2932.31 cm^{-1} for =C-H stretching, 1509.15 cm^{-1} for N-H bending, 3405.39 cm^{-1} strong and broad band for O-H stretching,1483.94 cm^{-1} and 1381.58 cm^{-1} for asymmetric and symmetric bending vibration of CH_3 group respectively also 1335.08 cm^{-1} represents the asymmetric vibration for S=O while 775.98 cm^{-1}, 548.13 cm^{-1} and 519.24 cm^{-1} are the absorption bands of out of plane for C=C of benzene ring,1229.9 cm^{-1} bending vibration for C-H, 1154.01 cm^{-1} for C-F stretching vibrations.

The following figures show representative examples (also for space consideration) of the spectra of each of the excipients alone or as a physical mixture with RVC (Figs. 5-8).

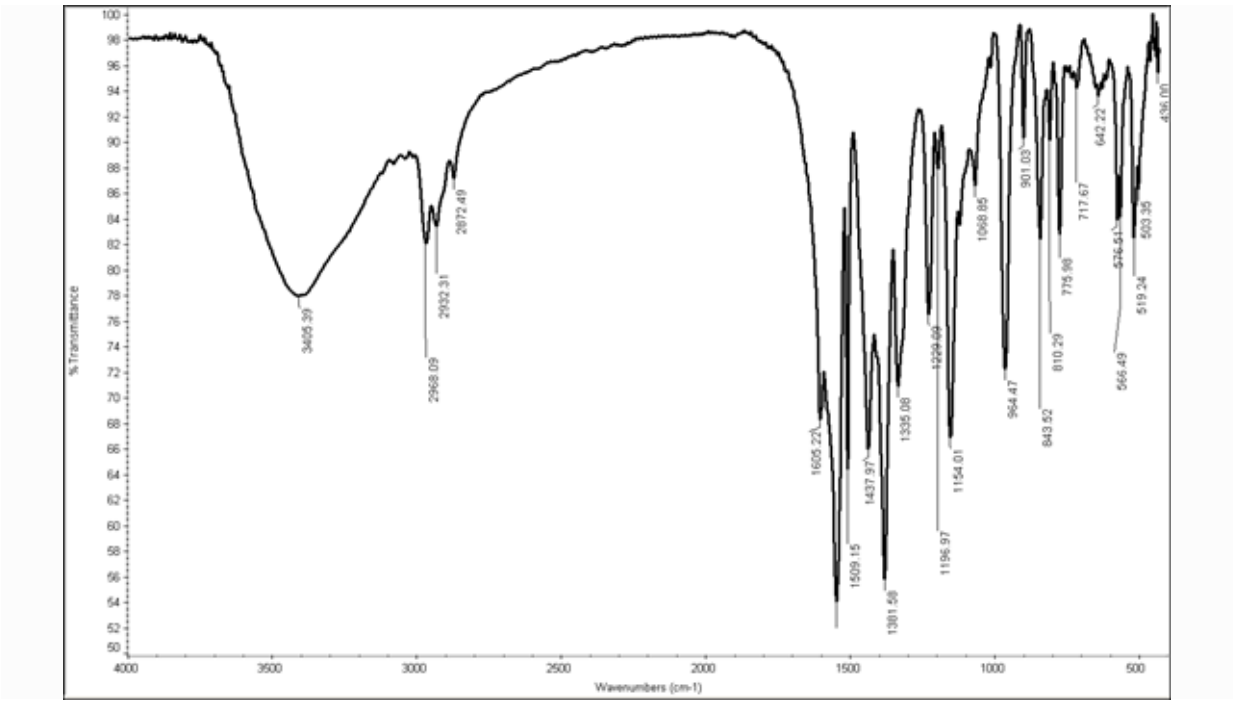

Fig. 4: The FT-IR spectrum of rosuvastatin calcium (RVC).

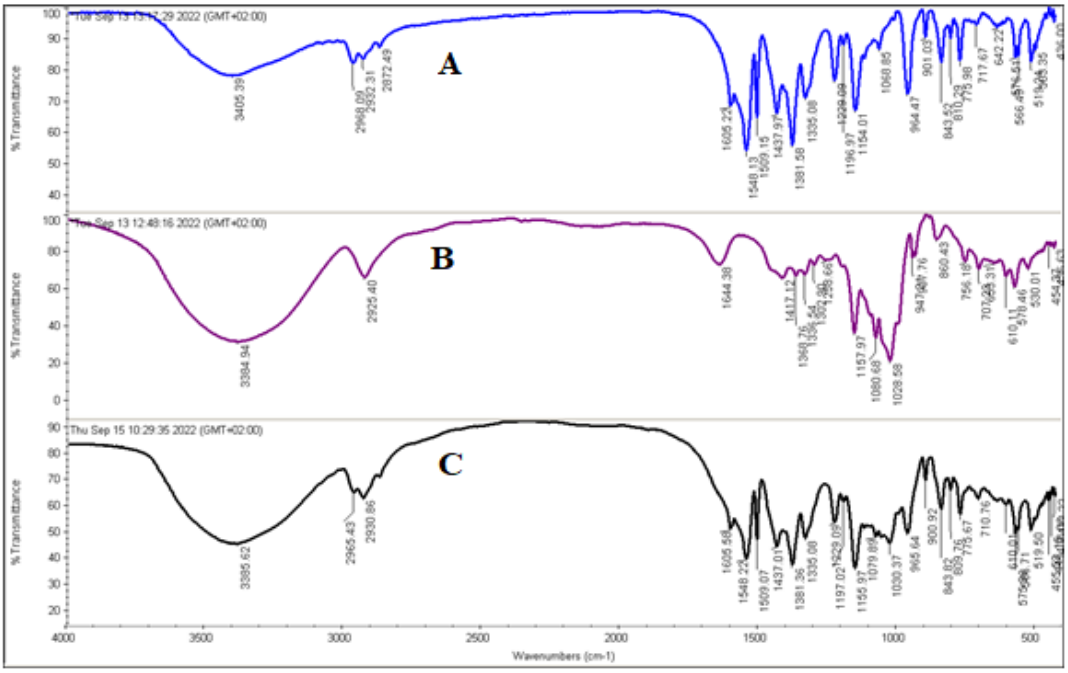

Fig. 5: FT-IR spectra of (A) rousvastatin calcium, (B) β-cyclodextrin and (C) their physical mixture.

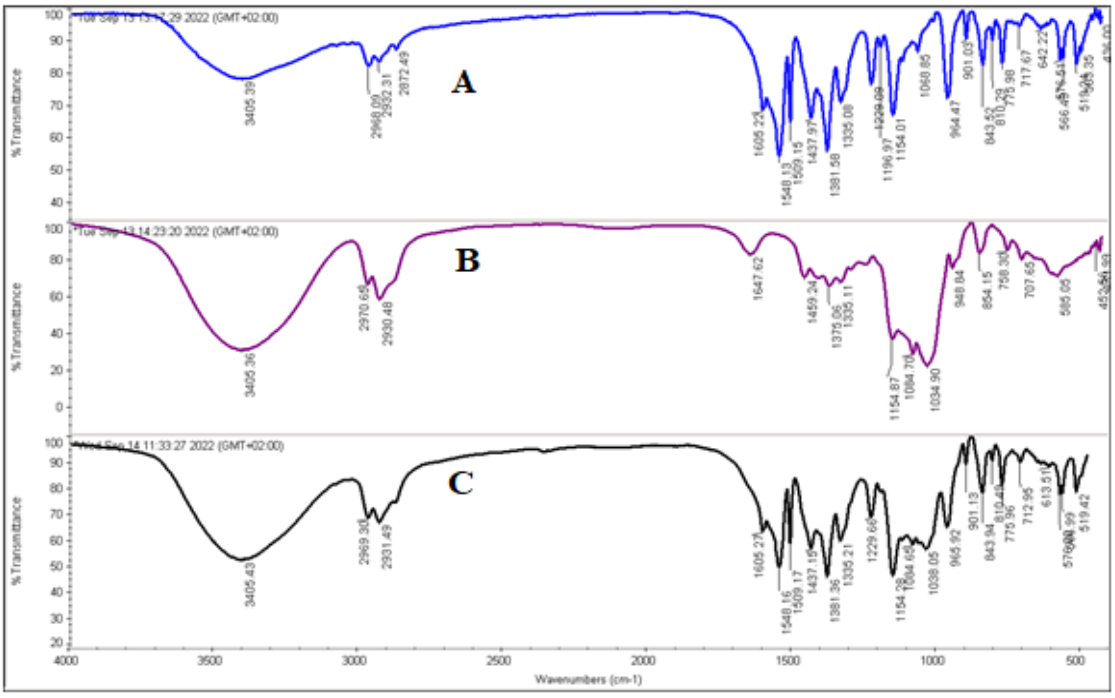

Fig. 6: FTIR spectra of (A) rousvastatin calcium, (B) hydroxylpropyl β-CD (HPβ-CD) and (C) their physical mixture.

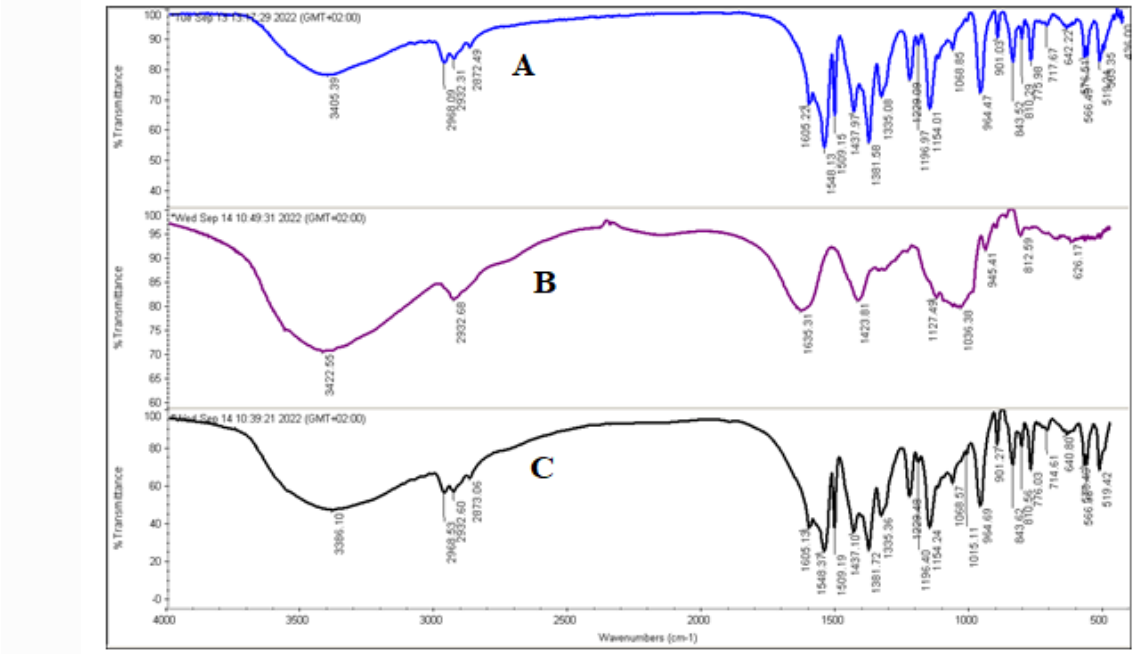

Fig. 7: FT-IR spectra of (A) rousvastatin calcium, (B) sodium alginate and (C) their physical mixture.

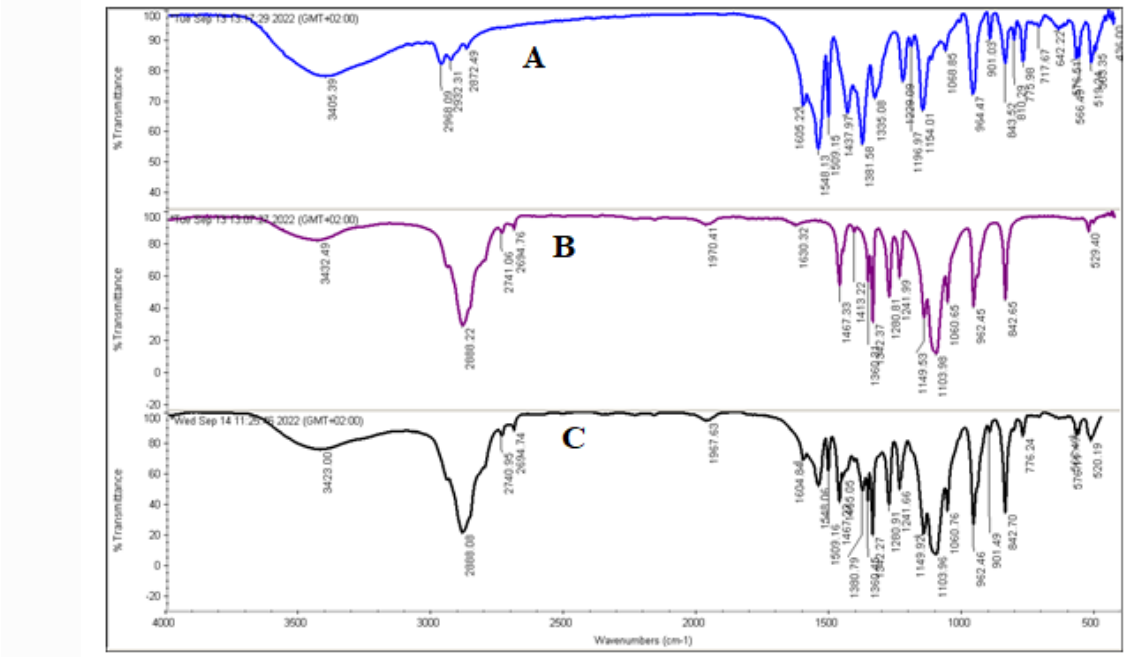

Fig. 8: FT-IR spectra of (A) rousvastatin calcium, (B) PEG 6000 and (C) their physical mixture.

The structural characterization of the polymers and their physical mixtures with the drug was performed by recording FT-IR spectra of the samples, figures 4-8, the spectra of RVC, excipient and RVC/excipient physical mixtures revealed that the characteristic bands of the drug or each of the excipients were maintained and no new bands appeared indicating the absence of interaction between the drug and the excipients. Similar results were also observed for all the excipients used in capping of AgNPs in this work.

Characterization of silver nanoparticles

Among various electron microscopy techniques, TEM uses transmitted electrons (electrons that are passing through the sample) to create an image. Hence, TEM offers valuable information on the morphology and inner structure of the sample particles[29&30].

Figure 9 shows the transmission electron microscopy (TEM) images of AgNPs prepared using sodium alginate (A) and β-CD (B) as capping (coating) agents. It is obvious that AgNPs prepared using β-CD are more to spherical in shape and have less size variation compared to those due to sodium alginate. Magnifying the TEM images clearly revealed smoother surfaces of AgNPs coated with β-CD compared with those coated with sodium alginates. In terms of particle sphericity, particle size distribution and surface topography, PEG 6000 coated AgNPs (C) occupied a medium way between AgNPs coated with β-CD and sodium alginate.

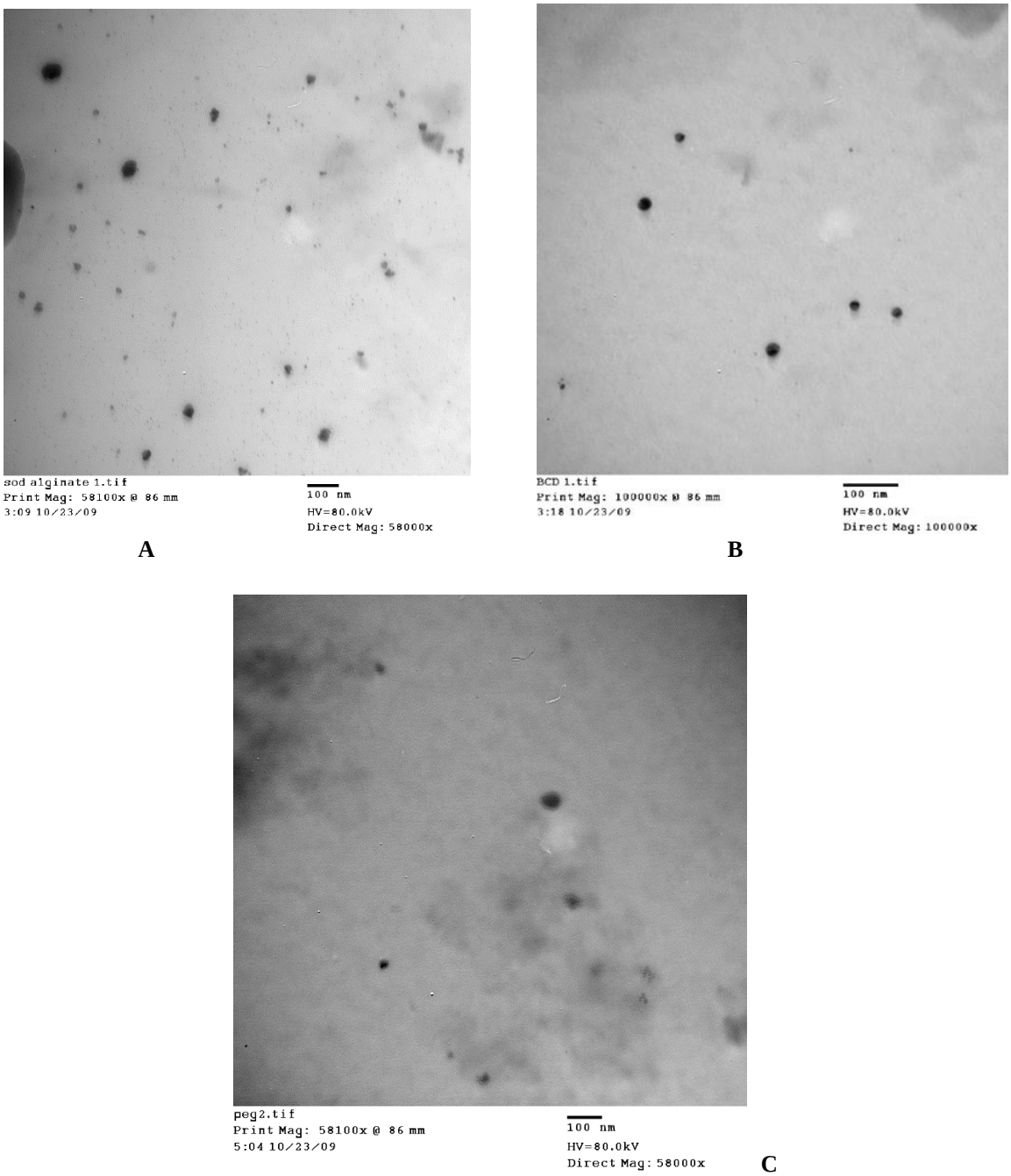

Fig. 9: Transmission electron microscopy of AgNPs prepared using sodium alginate (A), β-CD (B) and PEG6000 (C) as capping gents.

Zeta potential characterization of AgNPs was carried out in order to identify the physical stability of the nanoparticles and their size ranges. Table 1 shows these values.

Polydispersity index (PDI) is basically a representation of the distribution of size populations within a given sample. The value of PDI may vary from 0.01 (monodisperse particles) to 0.7, whereas value >0.7 indicates broad particle size distribution. Table 1 shows acceptable values of all systems except AgNPs coated with sodium alginate and to a lesser extent that coated with HPβ-CD. The suitability of nanocarrier formulations for a particular route of drug administration depends on their average diameter, PDI and size stability, among other parameters[31]. The tendency of nanocarriers to accumulate in the target tissue depends on their physicochemical characteristics including particle size distribution. Successful formulation of safe, stable and efficient nanocarriers, therefore, requires the preparation of homogenous (monodisperse) populations of nanocarriers of a certain size[31].

The NPs hydrodynamic diameter and zeta potential were analyzed on the Zetasizer aforementioned in the experimental part operating at a light source wavelength of 633 nm and a fixed scattering angle of 173°. The mean diameter determined by the zeta potential analyzer for AgNPs coated with the three aforementioned polymers (which have highest negative zeta potential) have the smallest particle mean diameter, as shown in table 1. In terms of physical stability and surface area, these three systems would be preferred in the assumed future formulation of RVC.

Figure 10 is a representative example of the investigated capping agents; PVP K90, which has the lowest values of PDI and particle mean diameter as shown in table 1.

Table 1: Mean diameter, polydispersity index and zeta potential values of silver nanoparticles synthesized using different capping agents.

AgNPs capping Agent	Mean diameter (nm)	Polydispersity index (PDI)	Zeta potential (mV)
Polyethylene glycol 6000	812.1	0.557	-13.7
Polyviylpyrrolidone K90	184.7	0.403	-10.5
Sodium alginate	245.2	1.000	-32.8
Polyvinyl alcohol	332.5	0.521	-28.6
β-cyclodextrin	796.6	0.558	-11.2
Hydroxylpropyl β-cyclodextrin	316.8	0.886	-25.4

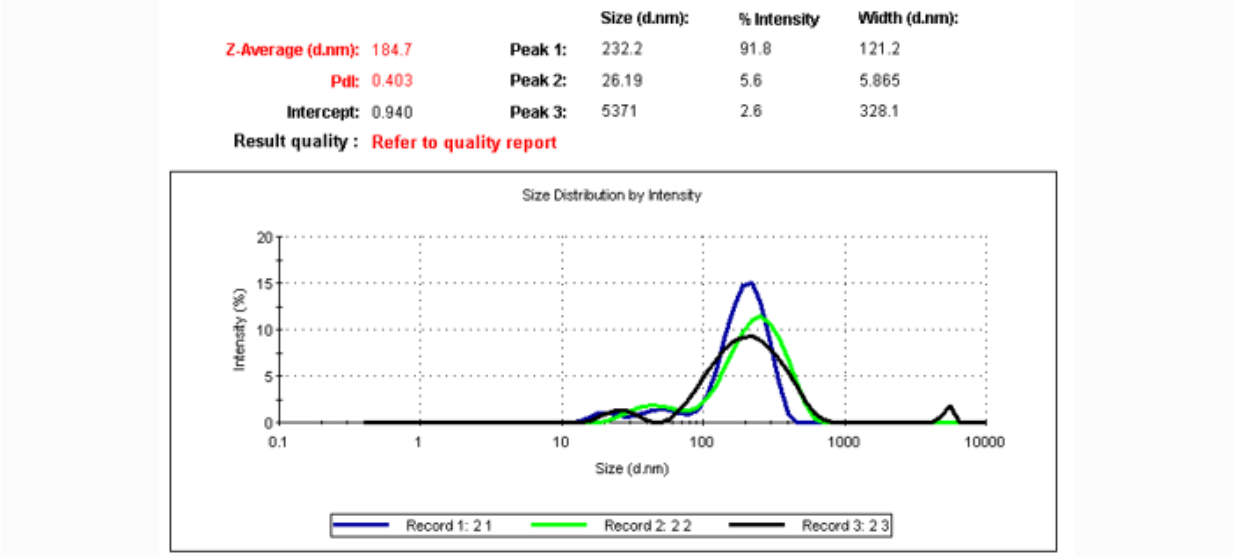

Fig. 10: Zetasizer measurement of mean diameter and polydispersity index of AgNPs coated with polyvinylpyrrolidone K90.

The effects of the observed mean size and PDI will be discussed later on the part of this work dealing with the antiinflammatory effects of AgNPs/RVC formulations.

The surface charges of the synthesized AgNPs were determined by zeta-potential measurements. It has been reported that the NPs which possess zeta-potential values more than +30 mV and less than –30 mV are relatively stable[32]. As shown in table 1, three coating polymers namely; sodium alginate, polyvinyl alcohol and HPβ-CD exhibit the highest values of negative zeta potential indicating acceptable stability.

Most examples from the literature suggest that an essential condition to improve the antibacterial efficacy of AgNPs is to have a positive particle surface charge. In fact, the positive charge allows for more efficient electrostatic interaction with the negative charges of the bacterial cell wall[33]. However, this expected effect obviously contrasted with many experimental data and represents a further important advantage of antibacterial NPs in terms of safety in mammalian cells and tissues assuming that cationic NPs are more cytotoxic than those with neutral or negative surface charge[34]. For example, Salvioni *et al.*[35] have found that AgNPs with negative surface charge, –18.3 mV as determined by zeta potential, have excellent antibacterial activity against both Gram positive and Gram negative bacteria.

Drug Loading and encapsulating efficiency of rousvastatin on silver nanoparticles

Table 2 shows the parameters is drug loading on the nanoparticles which is defined as the mass ratio of drug to drug-loaded nanoparticles. The results suggest that drug loading capacity and encapsulation efficiency (EE) are generally higher when the coating agents were polyhydroxy compounds. The significantly higher efficiency of HP-βCD compared loading of RVC on AgNPs coated with different agents according to the method and Eq. 1 explained in the experimental part. One of the key to β-CD may be attributed to the lower water solubility and complexing capacity of the latter.

Currently, most nanoparticles have relatively low drug EE (<10 wt.%), and developing methods to increase EE remains a challenge[36]. It is widely thought that drug EE >10% is acceptable. The EE shown in table 2 may be considered sufficient taking in account the relatively low dose of RVC as hypolipidemic drug. An exception is PVPK90 coated AgNPs which failed to load any drug.

As shown in table 2, the loading of RVC calculated per mg sliver in the nanoparticles ranged from approx. 26 to 1 mg. Taking in consideration the lowest peroral dose of RVC as antihyperlipidemic agent which is only 10 mg, an effective amount can be loaded using reasonable amount of AgNPs even for the least loading capacity in the β-cyclodextrin system. In all the listed systems in table 2, the amount of AgNPs was calculated and found equal to 0.1296 mg.

Table 2: Loading capacity and % encapsulation efficiency of rousvastatin calcium (RVC) on AgNPs coated with different agents.

Coating agent	Total drug added mg	Drug loaded mg	Drug loading capacity (mg/mg Ag nanoparticles)	%encapsulation Efficiency (% EE)
Hydroxylpropyl β-CD	6.2	3.4	26.15	54.8
Polyvinyl alcohol	6.5	3.1	23.85	47.7
Polyethylene glycol 6000	5.2	1.6	12.31	30.7
Sodium alginate	5.4	0.25	1.92	4.7
β-cyclodextrin	5.7	0.14	1.08	2.4
Polyviylpyrrolidone K90	6.1	0.00	0.00	0.0

Conclusion

Silver nanoparticles prepared by reduction of sliver nitrate and coated using different compatible capping agents were found to be near spherical in shape. The particle size and size homogeneity was dependent on the type of the capping agent used. For most of the systems investigated, the zeta potential values indicate good physical stability of the nanoparticles. The encapsulation efficiency and loading capacities of rousvastatin calcium on the prepared nanoparticles were also found to be variable depending on the capping agent.

REFERENCES

1- M. S. Arayne, N. Sultana, F. Qureshi, "Nanoparticles in delivery of cardiovascular drugs", ***Pak. J. Pharm. Sci.,*** 2007, 20 (4), 340-348.

2- J. K. Patra, K-H. Baek, "Green nanobiotechnology: Factors affecting synthesis and characterization techniques", ***J. Nanomater.,*** 2014, 2014, 1-12.

3- R. R. Joseph, S. S. Venkatraman, "Drug delivery to the eye: What benefits do nanocarriers offer?", ***Nanomedicine,*** 2017, 12, 683-702.

4- G. R. Rudramurthy, M. K. Swamy, U. R. Sinniah, A. Ghasemzadeh, "Nanoparticles: Alternatives against drug-resistant pathogenic microbes", ***Molecules,*** 2016, 21 (7), 1-30.

5- N. Martinho, C. Damgé, C. P. Reis, "Recent advances in drug delivery systems", ***J. Biomater. Nanobiotechnol.,*** 2011, 2 (5), 510-526

6- H. Jahangirian, E. G. Lemraski, T. J. Webster, R. Rafiee-Moghaddam, Y. Abdollahi, "A review of drug delivery systems based on nanotechnology and green chemistry: Green nanomedicine", ***Int. J. Nanomed.,*** 2017, 12 (12), 2957-2978.

7- I. Lampe, D. Beke, S. Biri, I. Csarnovics, A. Csik, Z. Dombradi, P. Hajdu, V. Hegedus, R. Racz, I. Varga, *et al.*, "Investigation of silver nanoparticles on titanium surface created by ion implantation technology", ***Int. J. Nanomed.,*** 2019, 14, 4709-4721.

8- M. Rafique, M. S. Rafique, U. Kalsoom, A. Afzal, S. H. Butt, A. Usman, "Laser ablation synthesis of silver nanoparticles in water and dependence on laser nature", ***Opt. Quantum Electron.,*** 2019, 6, 51-85.

9- H. J. Han, T. Yu, W. S. Kim, S. H. Im, "Highly reproducible polyol synthesis for silver nanocubes", ***J. Cryst. Growth,*** 2017, 469, 48-53.

10- Î. I. Kuntyi, A. R. Kytsya, I. P. Mertsalo, A. S. Mazur, G. I. Zozula, L. I. Bazylyak, R. V. Òopchak, "Electrochemical synthesis of silver nanoparticles by reversible current in solutions of sodium polyacrylate", ***Colloid. Polym. Sci.,*** 2019, 297, 689-695.

11- O. Gherasim, R. A. Puiu, A. C. Bîrca, A. C. Burdușel, A. M. Grumezescu, "An updated review on silver nanoparticles in biomedicine", ***Nanomaterials (Basel),*** 2020, 10 (11), 2318. doi: 10.3390/ nano10112318.PMID: 33238486; PMCID: PMC7700255.

12- J. Auclair, P. Turcotte, C. Gagnon, C. Peyrot, K. J. Wilkinson, F. Gagné, "The influence of surface coatings on the toxicity of silver nanoparticle in rainbow trout", ***Comp. Biochem. Physiol. C: Toxicol. Pharmacol.,*** 2019, 226 (12), 108623.

13- A. N. Zelikin, R. M. Zucker, J. Ortenzio, L. L. Degn, J. M. Lerner, W. K. Boyes, "Biophysical comparison of four silver nanoparticles coatings using microscopy, hyperspectral imaging and flow cytometry", ***PLoS ONE,*** 2019, 14, 1-24.

14- D. Acharya, K. M. Singha, P. Pandey, B. Mohanta, J. Rajkumari, L. P. Singha, "Shape dependent physical mutilation and lethal effects of silver nanoparticles on bacteria", ***Sci. Rep.,*** 2018, 8 (1), 201-208.

15- M. Y. Alkawareek, S. R. Abulateefeh, A. M. Alkilany, "Synergistic antibacterial activity of silver nanoparticles and hydrogen peroxide", ***PLoS ONE,*** 2019, 8, 1-12.

16- Z. Song, Y. Wu, H. Wang, H. Han, "Synergistic antibacterial effects of curcumin modified silver nanoparticles through ROS-mediated pathways", ***Mater. Sci. Eng. C,*** 2019, 99, 255-263.

17- H. M. Tawfeek, M. A. Younis, B. N. Aldosari, A. S. Almurshedi, A. Sunhat, A.

Abdelfattah, J. A. Abdel-Aleem, "Impact of the functional coating of silver nanoparticles on their *in-vivo* performance and biosafety", ***Drug Dev. Ind. Pharm.,*** 2023, 27 (5), 1-8.

18- O. Al Rugaie, A. A. H. Abdellatif, M. A. El-Mokhtar, M. A. Sabet, A. Abdelfattah, M. Alsharidah, M. Aldubaib, H. Barakat, S. M. Abudoleh, K. A. Al-Regaiey, *et al.*, "Retardation of bacterial biofilm formation by coating urinary catheters with metal nanoparticle-stabilized polymers", ***Microorganisms,*** 2022, 10, 1297-13010.

19- A. A. H. Abdellatif, H. N. H. Alturki, H. M. Tawfeek, "Different cellulosic polymers for synthesizing silver nanoparticles with antioxidant and antibacterial activities", ***Scientific Reports,*** 2021, 84 (11),1-18.

20- S. Zivkovic, G. Maric, N. Cvetinovic, D. Lepojevic-Stefanovic, B. Bozic Cvijan, "Anti-Inflammatory effects of lipid-lowering drugs and supplements-a narrative review", ***Nutrients,*** 2023 Mar 21, 15 (6), 1517. doi: 10.3390/ nu15061517. PMID: 36986246; PMCID: PMC10053759.

21- A. Choudhary, U. Rawat, P. Kumar, P. Mittal, "Pleotropic effects of statins: The dilemma of wider utilization of statin", ***Egypt. Heart J.,*** 2023, 75 (1), 1. doi: 10.1186/s43044-023-00327-8. PMID: 36602642; PMCID: PMC9816367.

22- V. Kumar, S. Dwajani, D. Gurjar, U. Pat, C. Vinodkumar, "Effect of rosuvastatin as an anti-inflammatory agent in albino rats", ***Asian J. Pharm. Clin. Res.,*** 4 (2), 2011, 74-76.

23- L. Alagić-Džambić, S. Omerović, M. Džambić, "Antimicrobial activity of rosuvastatin", ***IJPT,*** 2015, 6 (4), 7587-7592.

24- L. Mulfinger, S. D. Solomon, M. Bahadory, V. J. Aravindan, A. R. Susan, C. Boritz, "Synthesis and study of silver nanoparticles", ***Journal of Chemical Education,*** 2007, 84 (2), 322-331.

25- N. M. Elbaz, L. Ziko, R. Siam, M. Mamdouh, "Core-shell silver/polymeric nanoparticles-based combinatorial therapy against breast cancer *in-vitro*", ***Scientific Reports,*** 2016. 6, 30729-30738.

26- A. Shalviri, H. K. Chan, G. Raval, M. J. Abdekhodaie, Q. Liu, H. Heerklotz, X. Y. Wu, "Design of pH-responsive nanoparticles of terpolymer of poly(methacrylic acid), polysorbate 80 and starch for delivery of doxorubicin", ***Colloids and Surfaces B: Biointerfaces,*** 2013, 101, 405-413.

27- M. Tomassetti, A. Catalani, V. Rossi, S. Vecchio, "Thermal analysis study of the interactions between acetaminophen and excipients in solid dosage forms and in some binary mixtures", ***Journal of Pharmaceutical and Biomedical Analysis,*** 2005, 37 (5), 949-955.

28- O. S. Salih, L. H. Samein, W. K. Ali, "Formulation and *in-vitro* evaluation of rosuvastatin calcium niosomes", ***Int. J. Pharm. Pharm. Sci.,*** 2013, 5, Suppl 4, 525-535.

29- P. C. Lin, S. Lin, P. C. Wang, R. Sridhar, "Techniques for physicochemical characterization of nanomaterials", ***Biotechnol. Adv.,*** 2014, 32, 711-726.

30- H. Fissan, S. Ristig, H. Kaminski, C. Asbach, M. Epple, "Comparison of different characterization methods for nanoparticle dispersions before and after aerosolization", ***Anal. Methods,*** 2014, 6, 7324-7334.

31- M. Danaei, M. Dehghankhold, S. Ataei, F. Hasanzadeh Davarani, R. Javanmard, A. Dokhani, S. Khorasani, M. R. Mozafari, "Impact of particle size and polydispersity index on the clinical applications of lipidic nanocarrier systems", ***Pharmaceutics,*** 2018, 18 (5), 1-17.

32- B. Sundararajan, G. Mahendran, R. Thamaraiselvi, B. D. Ranjitha, "Biological activities of synthesized silver nanoparticles from *Cardiospermum halicacabum L.*", ***Bulletin of Materials Science,*** 2016, 39 (2), 423-431.

33- W. Li, X. Xie, Q. Shi, S. Duan, S. Ouyang, B. Chen, "Antibacterial effect of silver nanoparticles on *Staphylococcus aureus*", ***Biometals,*** 2011, 24 (1), 135-141.

34- J. Yang, J. Y. Lee, H. P. Too, "A general phase transfer protocol for synthesizing alkylamine-stabilized nanoparticles of noble metals", ***Anal. Chim. Acta.,*** 2007, 588 (1), 34-41.

35- E. Salvioni, V. Galbiati, S. Alessio, F. Avvakumova, D. Tortora, M. Prosperi, "Negatively charged silver nanoparticles with potent antibacterial activity and reduced toxicity for pharmaceutical preparations", ***International Journal of Nanomedicine,*** 2017, 12, 2517-2530.

36- G. Liu, S. Jin, L. C. Zhao, "Development of high-drug-loading nanoparticles", ***Chempluschem.,*** 2020, 85 (9), 2143-2157.

Sphinx Journal of Pharmaceutical and Medical Sciences, Vol. 5, Issue 1, 2023, pp. 33-46.

SJPMS

Sphinx Journal of Pharmaceutical and Medical Sciences

e-mail: sjpms@sphinx.edu.eg

SPHINX UNIVERSITY

جزيئات الفضة النانوية المغلفة بمختلف المركبات: التخليق الكيماوي والتوصيف والتحميل بعقار روزفاستاتين الكالسيوم

أحمد سيد إبراهيم[١] – أحمد السيد أبوطالب[٢] – محروس عثمان أحمد[٢،٣] – جيلان عبد الرازق عبدالعليم[٢]

[١]قسم الصيدلانيات ، كلية الصيدلة ، جامعة سفنكس ، أسيوط الجديدة ١٠ ، مصر

[٢]قسم الصيدلة الصناعية ، كلية الصيدلة ، جامعة اسيوط ، أسيوط ٧١٥٢٦ ، مصر

[٣]حاليا عميد كلية الصيدلة ، جامعة ميريت ، مدينة سوهاج الجديدة ٨٢٥١١ ، مصر

أجري هذا البحث بهدف صياغة عقار الروزفاستاتين باستخدام جسيمات الفضة النانوية كحامل للعقار ، وذلك للاستفادة من خصائص هذه الجسيمات من حيث المساحة السطحية الكبيرة ، وقد ثبت من المسح الحرارى التفاضلي وطريقة فوريه للأشعة تحت الحمراء أن العقار متوافق مع المواد المستخدمة في تغليف جسيمات الفضة النانوية ، وقد خلقت هذه الجزيئات باختزال نترات الفضة باستخدام بوروهيدرايد الصوديوم ، وفحصت خصائص الجسيمات باستخدام الميكروسكوبي الالكتروني النافذ للتعرف على شكلها وطبيعة أسطحها ، واستخدم فرق جهد زيتا لقياس مدى ثباتها ومتوسط احجامها ، وتم تحميل عقار روزفستاتين الكالسيوم على الجسيمات ، وقد اختلف شكل الجسيمات وحجمها وثباتها ومقدار تحميل العقار تبعا لنوع المادة المغلفة للجسيمات.